Analyst

Accepted Manuscript

ROYAL SOCIETY OF CHEMISTRY

www.rsc.org/analyst

Journal Name

RSCPublishing

ARTICLE

Fluorescent turning on detection of Sn^{2+} in living eukaryotic and prokaryotic cells

Cite this: DOI: 10.1039/x0xx00000x

Haichuang Lan,[a] Ying Wen,[a] Yunming Shi,[b] Keyin Liu,[a] Yueyuan Mao,[a] and Tao Yi*[a]

Received ooth January 2012,
Accepted ooth January 2012

DOI: 10.1039/x0xx00000x

www.rsc.org/

Sn^{2+} was usually added to toothpaste to prevent dental plaque and oral disease. However, studies of its physiological role and bacteriostatic mechanism are restricted by the lack of versatile Sn^{2+} detection methods applicable to living cells and Streptococcus mutans. Here we report two Sn^{2+} fluorescent probes containing rhodamine B derivative as a fluorophore, linked via amide moiety to N, N-bis(2-hydroxyethyl)ethylenediamine (**R1**) and tert-butyl carbazate group (**R2**), respectively. These probes can selectively chelate Sn^{2+} and show marked fluorescent enhancement due to the ring open reaction of rhodamine induced by Sn^{2+} chelating. The probes have high sensitivity and selectivity for Sn^{2+} in the presence of various relevant metal ions. Particularly, both **R1** and **R2** can target lysosome and **R2** can probe Sn concentrations in lysosomes with rather acidic microenvironment. Furthermore, the two probes have low toxicity and can be used as imaging probes for monitoring Sn^{2+} not only in living KB cell (eukaryotic cell) but also streptococcus mutans (prokaryotic cell), which is a useful tool to study the physiological function of Sn^{2+} in biological systems.

Introduction

Sn^{2+} has been used in dentistry since the 1950s as a chemical adjunct to prevent dental caries.[1] Sn^{2+} was found to effectively inhibit streptococcus mutans, which lead to tooth decay in human interproximal dental plaque.[2] Recently, there has been increasing interest in the biological roles of Sn^{2+} because Sn is an essential trace mineral for humans and is found in the greatest amount in the adrenal gland, liver, brain, spleen and thyroid gland.[3] There is some evidence that tin is involved in growth factors and cancer prevention of human beings. Deficiency of tin may result in poor growth and hearing loss, but excess tin accumulation can abhorrently affect respiratory and digestive systems.[4] However, studies of the physiological role and bacteriostatic mechanism of tin ion are restricted by the lack of versatile Sn^{2+} detection methods applicable to living cells and Streptococcus mutans. It is of great importance to establish a method for the determination of Sn in biological systems.

Some kinds of techniques have been developed for determination of Sn, such as flame atomic absorption spectrometry, potentiometric membrane sensor[6] and UV/visible spectrophotometric technique.[7] However; those methods are not suitable for in suit detection of Sn in biological systems. In the previous work, we have firstly developed a fluorescent chemosensor for Sn^{4+}, which was successfully applied in sensing Sn^{4+} in living cell.[8] Recently, Han's group reported another water soluble fluorescent chemosenor for Sn^{4+}, unfortunately, biological application of the probe was not explored.[9] There is a further need for a probe that minimizes background noise while providing high fluoresce intensity in living cells consistent where Sn^{2+} is found in the cell.

As we know, Rhodamine B is widely used as a fluorescent probe for the detection of mental ion[10] and biomolecule,[11] due to the ring opening reaction of rhodamine.[12] However, Rhodamine B is very sensitive to acidic environment; it is an advantage to have a probe that works well in pH conditions in an organelle that plays a role in Sn accumulation in the cell. Herein, two novel rhodamine B based fluorescent probes (**R1** and **R2** in Scheme 1) for Sn^{2+} were designed and synthesized. Compared with our previous probe, the new compounds are easier synthesized and have larger solubility, better selectivity and sensitivity for Sn^{2+}. Furthermore, **R1** and **R2** possess pithy flexible chain with acyl and hydroxy, which have more affinity for Sn^{2+} than other metal ions. Particularly, **R2** can work in a comparatively lower pH environment that can probe Sn concentrations in lysosomes with rather acidic microenvironment. The most important, **R1** and **R2** can detect Sn^{2+} both in living KB cells and streptococcus mutans by fluorescent turning on process. To the best of our knowledge, there is no report of a fluorescent probe for Sn^{2+} imaging in prokaryotic cell- streptococcus mutans.

Experiment

General methods

Unless otherwise noted, materials were obtained from commercial suppliers and were used without further purification. Rhodamine (95%) was obtained from Sinopharm Chemical Reagent Co., Ltd. (Shanghai). Other chemicals were provided from Shanghai No.1 chemical reagent. Flash chromatography was carried out on silica gel (200-300 mesh). The ^{1}H NMR (500 MHz) and ^{13}C NMR (125 MHz) spectra were recorded on a Bruker DRX-500 spectrometer. Proton chemical shifts are reported in parts per million downfield from tetramethylsilane (TMS). HRMS was obtained on an LTQ-Orbitrap mass spectrometer (ThermoFIsher, San Jose, CA). UV-Vis spectra were recorded on a Shimadzu UV-2250 spectrophotometer. Fluorescence spectra were recorded on an Edinburgh FLS-920 spectrophotometer. All pH measurements were made with a model Mettler-Toledo meter.

Synthesis of sensors

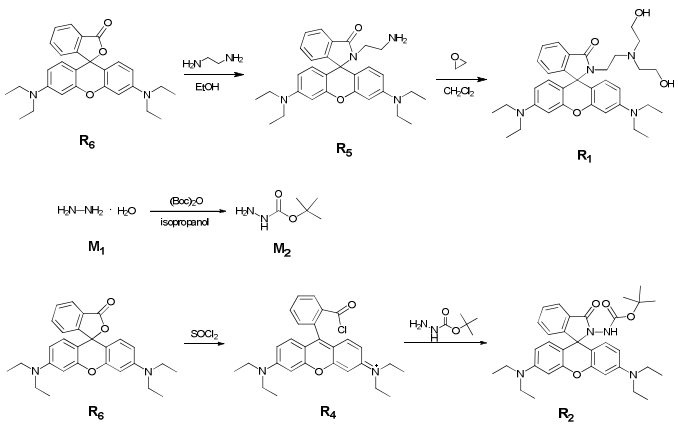

Scheme 1 Synthesis of **R1** and **R2**

The synthesis process of **R1** and **R2** is shown in scheme 1. The procedure for the synthesis of **R5** is described in the literature.[13] **R1** was prepared by treatment of **R5** with excess oxirane to give the diol.[14] Hydrazine monohydrate was protected by Boc to affording **M2**.[15] Treatment of **M2** with rhodamine B acid chloride gave fluorescent probe **R2**.[16] The details of synthesis is shown in ESI†.

Metal ion sensing procedures

The solutions of the metal ions (10.0 mM) were prepared in deionized water. A stock solution of **R1**, **R2** (0.2 mM) was prepared in ethanol and was then diluted to 20 μM with ethanol–water (1: 1, v/v, pH 7.04) for spectral measurement. In titration experiments, each time a 2.0 mL solution of **R1**, **R2** (20 μM) was filled in a quartz optical cell of 1 cm optical path length, and the Sn^{2+} stock solution was added into the quartz optical cell gradually by using a micro-pipette. Spectral data were recorded at 5 min after the addition. In selectivity experiments, the test samples were prepared by placing appropriate amounts of metal ion stock into 2.0 mL solution of **R1**, **R2** (20 μM). For fluorescence measurements, excitation was provided at 560 nm, and emission was collected from 565 to 700 nm.

pH titration of R1, R2

Stock solution of **R1** and **R2** were respectively added to sodium phosphate buffers of various pH to a final concentration of 10 μM. The fluorescence emission spectra were recorded as a function of pH using λ_{ex} at 560 nm. The titration curves were plotted by fluorescence emission intensities at 580 nm versus pH.

Cell culture

The KB cell line was provided by Institute of Biochemistry and Cell Biology, Shanghai Institutes for Biological Sciences (SIBS), Chinese Academy of Sciences (CAS) (China). Cells were grown in MEM (Modified Eagle's Medium) supplemented with 10% FBS (Fetal Bovine serum) and 5% CO_2 at 37 ºC. Cells (5×10^{-8} L^{-1}) were plated on 18 nm glass coverslips and allowed adhere for 24 hours.

Bacterial culture

The "streptococcus mutans" (ATCC® 700610™) was prepared by inoculating the single colony from the BHI agar plate into 5 mL BHI broth and incubating at 37°C for 48 h.

Fluorescence imaging

Confocal fluorescence imaging was performed with an OLYMPUS IX81 laser scanning microscope and a 60 × oilimmersion objective lens. The microscope was equipped with multiple visible laser lines (405, 488, 543 nm). Images were collected and processed with Olympus FV10-ASW software.

For fluorescence imaging of intracellular Sn^{2+}: (1) 10 μM **R1** or **R2** in the culture media containing 0.2% (v/v) DMSO was added to the cells. The cells were incubated at 37 °C for 30 min, and washed with PBS three times to remove the excess probe and bathed in PBS (2 mL) before imaging. (2) After washing with PBS (2 mL × 3) to remove the excess probe, the cells were treated with 50 μM SnF_2 for 30 min. Excitation of **R1** or **R2** loaded cells at 543 nm was carried out with a semiconductor laser, and emission was collected at 560–660 nm (single channel). (3) 50 μM SnF_2 in the culture media was added to the cells. The cells were incubated at 37 °C for 30 min, and washed with PBS three times to remove the excess SnF_2. After washing with PBS (2 mL × 3) to remove the excess SnF_2, the cells were treated with 10 μM **R1** or **R2** separately for 30 min, and washed with PBS three times to remove the excess probe and bathed in PBS (2 mL) before imaging. Cell imaging was then carried out as the former.

For lysosome colocalization experiments: (1) 10 μM **R1** or **R2** in the culture media containing 0.2% (v/v) DMSO was added to the cells. The cells were incubated at 37°C for 30 min, and washed with PBS three times to remove the excess probe and bathed in PBS (2 mL) before imaging. (2) After washing

with PBS (2 mL × 3) to remove the excess probe, the cells were treated with 50 μM SnF_2 at 37 °C for 30 min, and washed with PBS three times to remove the excess SnF_2 and bathed in PBS (2 mL) before imaging. (3) After washing with PBS (2 mL × 3) to remove the excess SnF_2, the cells were treated with 1.0 μM LysoTracker® Green DND at 37 °C for 30 min. The cells were filled with 2 mL of PBS for fluorescence imaging equipped with the appropriate excitation and emission filters for **R1** or **R2** (λ_{ex} = 543 nm, λ_{em} = 560−660 nm), Lysotracker Green (λ_{ex} = 488 nm, λ_{em} = 500−540 nm). (4) 50 μM SnF_2 in the culture media was added to the cells. The cells were incubated at 37 °C for 30 min, and washed with PBS three times to remove the excess SnF_2. After washing with PBS (2 mL × 3) to remove the excess SnF_2, the cells were treated with 10 μM **R1** or **R2** separately for 30 min, and washed with PBS three times to remove the excess probe and bathed in PBS (2 mL) before imaging. Cell imaging was then carried out as the former. (5) After washing with PBS (2 mL × 3) to remove the excess probes, the cells were treated with 1.0 μM LysoTracker® Green DND at 37 °C for 30 min. Cell imaging was then carried out as the former.

For fluorescence imaging of Sn^{2+} in bacteria: Freshly diluted streptococcus mutans (ATCC® 700610™) was sub cultured in the presence of the 10 μM **R1** or **R2**, separately at 37ºC on a shaker bed at 400 rpm for 60 min. Then the bacteria were collected by centrifugation at 8,000 rap for 2 min and rinsed with Saline (pH = 7.0), the process was repeated three times before imaging. After washing with Saline (2 mL × 3) to remove the excess probes, the bacteria was cultured in the presence of the 50 μM SnF_2 at 37 ºC on a shaker bed at 400 rpm for 60 min. Then the bacteria were collected by centrifugation at 8,000 rap for 2 min and rinsed with Saline (pH = 7.0), the process was repeated three times before imaging. The light source at 543 nm provided excitation and emission was collected in the range of 560-660 nm.

Cytotoxicity Assay

The in vitro cytotoxicity was measured using a standard methyl thiazolyl tetrazolium[17] (MTT, Sigma-Aldrich) assay in KB cell lines. Cells growing in log phase were seeded into 96-well cell-culture plate at 1×10^4/well. The chemosensor **R1** or **R2** (100 μL/well) at concentration of 1.0, 2.5, 5.0, 10.0, 25.0, 50.0, 100.0 μM was added to the wells of the treatment group, and 100 μL/well DMSO diluted in DMEM at final concentration of 0.2% to the negative control group, respectively. The cells were incubated for 24 and 48 h at 37ºC under 5% CO_2. The combined MTT/PBS solution was added to each well of the 96-well assay plate, and incubated for an additional 4 h. An enzyme –linked immunosorbent assay (ELISA) reader (infinite M200, Tecan, Austria) was used to measure the OD 490 (Absorbance value) of each well. The following formula was used to calculate the viability of cell growth.

Viability (%) = (mean of Absorbance value of treatment group/mean Absorbance value of control) ×100

Results and discussion

Metal ion response

Fluorescent 'turn on' probe is conducive for detection target. The solution of **R1** or **R2** (20 μM) in ethanol–water (1: 1, v/v, pH 7.04) were colourless without fluorescence. With addition of Sn^{2+} (0–20 eq) to the solution of **R1** or **R2**, the colour of the solution changed to pink and an orange fluorescence observed (Fig. 1). The emission titration experiment shows that the emission at 580 nm was turned on and grown drastically with an excitation of 560 nm light for both **R1** and **R2** due to the ring open reaction of rhodamine induced by Sn^{2+} chelating [8,9] (Fig. 1a and 1c). The fluorescent quantum yield (Q_F) increased from 0.076 to 0.237 for **R1** and 0.066 to 0.187 for **R2** by addition of Sn^{2+}. Corresponding titration absorption spectroscopy was carried out under the same condition. A new absorption peak at 560 nm gradually appeared for **R1** and **R2** with addition of Sn^{2+} (Fig 1b and 1d). At less than 20 eq of Sn^{2+}, an excellent linear correlation between the emission intensity (580 nm) of **R1** and **R2** and the Sn^{2+} concentration was obtained with $R_{\mathbf{R1}}^2$ = 0.96631 and $R_{\mathbf{R2}}^2$ = 0.99231, which indicated that the fluorescence intensity at 580 nm increased as a linear function of the Sn^{2+} concentration in this concentration range (insets of Fig. 1a and 1c). Although **R1** and **R2** possess same response model to Sn^{2+}, it is necessary to explore which one more sensitive for Sn^{2+}. The detection limit of **R1** and **R2** to Sn^{2+} was tested as 5.7×10^{-7} M and 4.6×10^{-7} M (Fig. S1), respectively, indicated that both chemosensors **R1** and **R2** were sensitive for detection of Sn^{2+}. Furthermore, the present two sensors are superior to that of previous reports. [18]

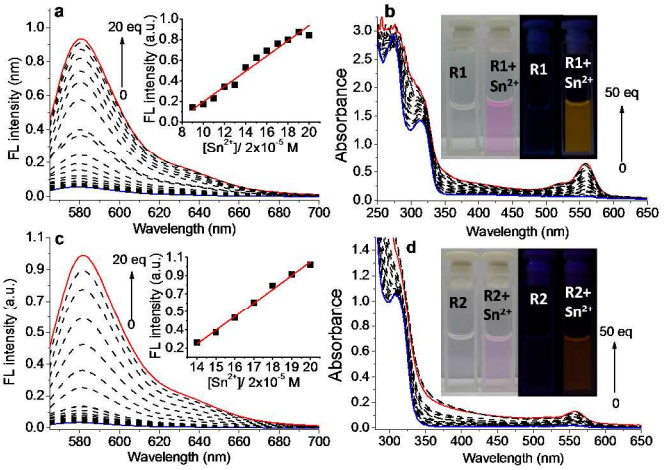

Fig. 1 Fluorescence spectra of (a) **R1** and (c) **R2** (20 μM) upon addition of 0–20 eq of Sn^{2+}; absorption spectra of (b) **R1** and (d) **R2** upon addition of 0–50 eq of Sn^{2+}; solvent condition: ethanol–water (1: 1, v/v), pH 7.04. The inset of (a) and (c) shows the emission intensities at 580 nm as a function of concentrations of Sn^{2+}, respectively; the inset of (b) and (d) shows the colour and fluorescence change of **R1** and **R2** with addition of Sn^{2+}, respectively.

High-level selectivity is of paramount importance for an excellent chemosensor. Both **R1** and **R2** show high selectivity on sensing Sn^{2+}. The solution of **R1** and **R2** (20 μM) in ethanol–water (1: 1, v/v, pH 7.04) were tuning on just in the

present of Sn^{2+} and Cr^{3+}, while other transition and heavy metal ions such as K^+, Ag^+, Ca^{2+}, Mg^{2+}, Zn^{2+}, Pb^{2+}, Ni^{2+}, Mn^{2+}, Co^{2+}, Cd^{2+}, Hg^{2+}, displayed minimal enhancement with an excitation of 560 nm (Fig 2). The data showed that the selectivity of **R2** is slightly worse that of **R1**. Photograph of fluorescence changes of **R1** and **R2** (2.0×10^{-5} M) upon addition of various metal ions (10 eq) were in Fig 2d. Although the detection of Sn^{2+} was interfered with Cr^{3+}, the selectivity has been improved compared with our previous work.[9]

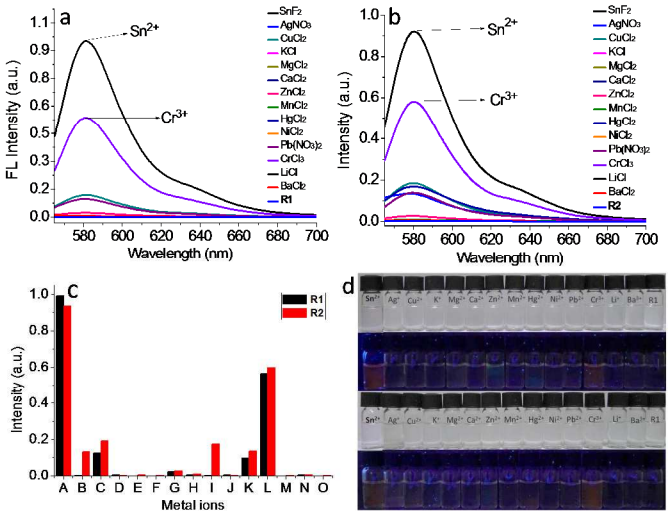

Fig. 2 Fluorescence spectral of (a) **R1** and (b) **R2** with addition of various metal ions in ethanol–water (1: 1, v/v, pH 7.04) solution (λ_{ex} = 560 nm); (c) the fluorescent intensity changes of **R1** (black) and **R2** (red) at 580 nm upon various metal ions; A, Sn^{2+}; B, Ag^{2+}; C, Cu^{2+}; D, K^+; E, Mg^{2+}; F, Ca^{2+}; G, Zn^{2+}; H, Mn^{2+}; I, Hg^{2+}; J, Ni^{2+}; K, Pb^{2+}; L, Cr^{3+}; M, Li^+; N, Ba^{2+}; O, blank; (d) photographs of the colour and fluorescence changes of **R1** (above) and **R2** (below) with addition of various metal ions (10 eq) in ethanol–water (1: 1, v/v, pH 7.04).

Besides high sensitivity and selectivity, a short response time is another necessity for a fluorescent probe to dynamically image intracellular Sn^{2+} ions or monitor Sn^{2+} in environmental samples in real time. To study the response time of the probes **R1** and **R2** to Sn^{2+}, the fluorescence enhancement of **R1** and **R2** at 580 nm with resting time after addition of Sn^{2+} (10 μM) was recorded, and results are shown in Fig. 3. The fluorescent signals increased with resting time at the beginning and reached to constant within 3 and 2 min, respectively, for **R1** and **R2** after addition of Sn^{2+}. This means that the two probes have quickly responds time towards Sn^{2+} and could be used for real-time tracking of Sn^{2+} in biological samples.

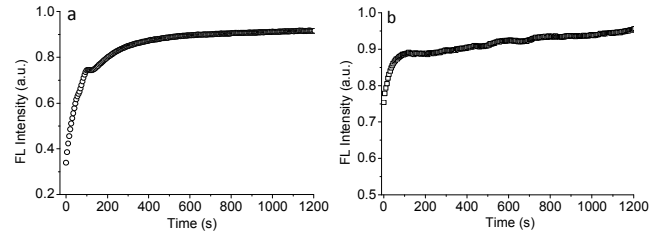

Fig. 3 Kinetics of the fluorescence enhancement of (a) **R1** and (b) **R2** (10 μM) at 580 nm in the presence of Sn^{2+} (10 μM) (λ_{ex} = 560 nm).

Sensing mechanism

In order to understand the binding stoichiometry of **R**-Sn^{2+} complexes, Job plot experiments were carried out as shown in Fig. 4. The emission intensities at 580 nm were plotted against the molar fraction of **R1** (Fig. 4a) and **R2** (Fig. 4b) with a constant total concentration of [**R**+Sn^{2+}] (2.0×10^{-5} M). Maximum emission intensities at 580 were reached when the molar fraction was 0.5 in both **R1** and **R2**, indicating the formation of 1:1 complexes between the probe and Sn^{2+} (Fig. 4c and 4d). The equilibrium constants (K) between **R1** (or **R2**) and Sn^{2+} were obtained by using nonlinear curve fitting.[19] On the basis of 1:1 stoichiometry, the K value of the complex between **R1** (or **R2**) and Sn^{2+} was estimated to be $K_{\mathbf{R1}} = 4.4\times10^4$ ($r^2 = 0.981$) and $K_{\mathbf{R2}} = 3.8\times10^4$ ($r^2 = 0.988$) (Fig. S2). The binding process between **R1** (or **R2**) and Sn^{2+} was further proven by Maldi-Tof-MS spectroscopy of the complex (Fig. S3). The mass data for a solution of **R1** + Sn^{2+} showed two peaks at m/z = 729.29, 727.29; calc. for $C_{34}H_{43}F_2N_4O_4Sn$ [**R1**+SnF_2–H^+], 729.23, 727.23. The mass data for **R2** + Sn^{2+} showed one peak at m/z = 737.37; calc. for $C_{33}H_{40}N_4O_4SnF_2Na$ [**R2**+SnF_2+Na^+]: 737.19.

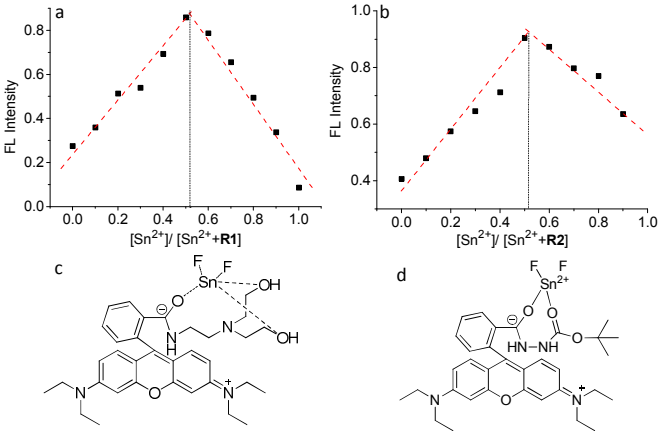

Fig.4 Job's plots of **R1** (a) and **R2** (b) for the emission intensity change at wavelength of 580 nm. The total concentration of **R1** (or **R2**) and Sn^{2+} was 20 μM. Proposed structure of complexes of (c) **R1**+Sn^{2+} and (d) **R2**+Sn^{2+}.

Impact of pH value on fluorescence

The pirolactam ring of the rhodamine derivatives will open in a certain pH range and indicates the fluorescence of rhodamine.[20] It is therefore necessary to check the fluorescent properties of **R1** and **R2** in solutions with different pH values. Furthermore, in cell, the acidity of different organelles is great disparity.[21] For example, the normal pH of lysosomes is 4.5-5.5, which may induce ring open of **R1** or **R2**.[22] Considering that the application of Sn^{2+} probe **R1** and **R2** intracellular or extracellular may be disturbed by the pH, the acid–base titration experiments were carried out by adjusting the pH with an aqueous solution of NaOH and HCl in Phosphate-Buffered Saline (PBS) (Fig. 5a and 5b). The titration revealed that the pH range for inducing **R1** or **R2** fluorescence turning on is 2.5-6 or 2-4.5, respectively. It is predicted that **R1** will be turned on by

lysosomes in cell without Sn^{2+} present, while **R2** can detect Sn^{2+} in a larger pH range.

The proposed mechanism for the fluorescence of **R1** and **R2** affected by pH is explained in Fig 5c. The mechanism of the fluorescence change is based on the change in structure between spirocyclic and open-cycle forms.[12] The spirocyclic form in high pH value is non-fluorescence. With the decrease of pH value in the range of 2.5~5.0, the spirocyclic form of both **R1** and **R2** was ring opened by H^+ with the fluorescence switched on due to the enlarged conjugate system (the formation of push-pull electronic structure). With further decrease of the pH value (pH<2.5), the N, N-dimethyl group of **R1** and **R2** was protonated, breaking the push-pull electronic structure, resulted in fluorescence off of the probes. Furthermore, due to the weak electron donating effect of the Boc protected NH group of **R2**, **R2** is more stable than **R1** in weak acidic environment.

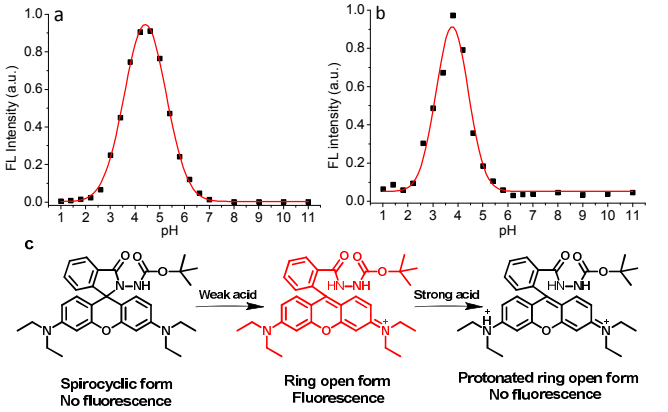

Fig. 5 Dependence of fluorescence at 580 nm of (a) **R1** and (b) **R2** (10 μM) on different pH in PBS solution (λ_{ex} = 560 nm). (c) The proposed mechanism for the fluorescence of **R1** and **R2** affected by pH.

Cytotoxicity of R1 and R2

An ideal celluar chemosensor for practical application should minimally perturb living systems at the concentration employed. Accordingly, the cytotoxicities of solvent **R1**, **R2** were determined using the MTT assay in KB cell. In the present of **R2** concentration of 1.0 –100.0 μM, the cellular viability were estimated to be greater than 90% (Fig. 6) after incubation for 24 h. **R1** also show low cellular toxicity in 24 h at a concentration of 1.0-10.0 μM. The results indicate that **R2** is less toxic than **R1**, more suitable for intracellular detection of Sn^{2+}.

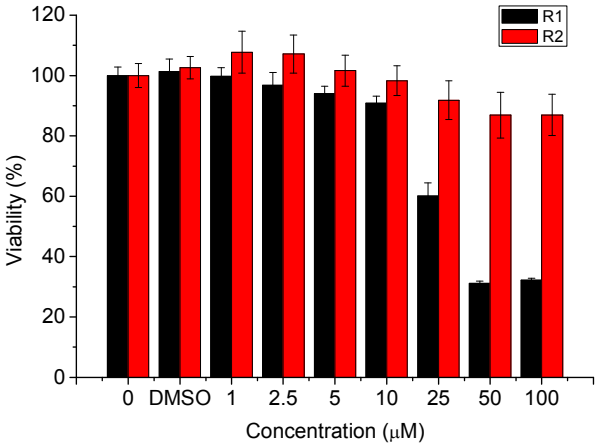

Fig. 6 Cell viability values (%) estimated in KB cell by MTT proliferation test versus concentrations (0-100 μM) of **R1** (black) and **R2** (red) after 24 h incubation at 37 °C.

Fluorescence imaging of intracellular Sn^{2+}

Sn^{2+} is usually added to toothpaste as inhibitory factor,[1] so oral epithelial cells are most likely to come into contact with Sn^{2+}. The KB cells are the best candidate for explored Sn^{2+} distribution in cell level by fluorescence imaging. Here the practical applicability of **R1** and **R2** as a Sn^{2+} probe in the fluorescence imaging of living KB cells was investigated. Firstly, the KB cells were separately stained with 10 μM **R1** or **R2** at 37 ºC for 30 min. As determined by confocal laser scanning microscopy (CLSM), **R1** gave fluorescence emission in a site of KB cells without Sn^{2+} present (Fig. 7, a1-g1); **R2** gave scarcely fluorescence (Fig. 7, a2-g2). This result confirmed our prediction in pH titration experiment which lysosomes acidity may induce **R1** fluorescence emission without Sn^{2+}. When the cells were supplemented with **R1** or **R2** in the PBS for 30 min at 37 ºC and then incubated with 50 μM Sn^{2+} under the same conditions, **R2** gave a significant fluorescence increasing from the certain intracellular region (Fig. 7, d2-h2); **R1** showed slightly changing in fluorescence intensity (Fig. 7, d1, h1). Cell imaging experiments indicate that **R2** is more suit for detection of Sn^{2+} in cell level, due to its less background noise, particularly in more acidic environments like lysosomes. Furthermore, **R1** and **R2** may be specificity targeting for lysosomes, because **R1** and **R2** bear the groups similar to 'dimethylethylamino' that is the targeting anchor for lysosomes.[21,22]

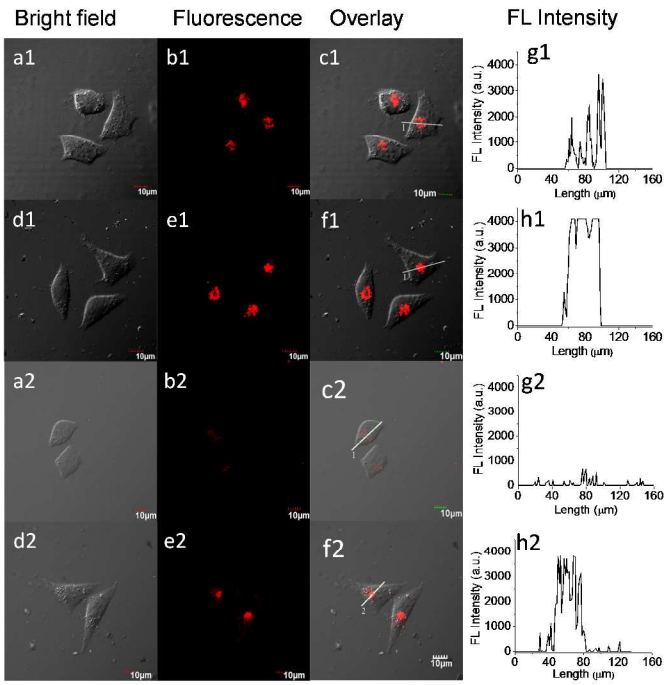

Fig. 7 CLSM images of KB cells. (a1-c1) and (a2-c2) Cells separately incubated with 10 μM **R1** and **R2** for 30 min, respectively; (d1-f1) and (d2-f2) followed incubated with 50 μM SnF_2 for 30 min, respectively. Emission was collected in red channel at 560–660 nm (b1, e1, b2, e2); a1, d1, a2, d2 are bright field images and c1, f1, c2, f2 are overlay images, respectively (λ_{ex} = 543 nm); g1, g2, h1 and h2 are the fluorescent intensity of the line on cells.

Lysosomes colocalization experiments

To probe the intracellular locations of **R1** or **R2**, KB cells were co-stained with **R1** or **R2**, Sn^{2+} and LysoTracker® Green DND, which is a commercially available marker for lysosomes and has good separation in excitation and emission spectra with **R1** and **R2**. As shown in Fig. 8, a1−d1, the fluorescence images between **R1** and lysotracker overlapped very well. This result verify our prediction in pH titration experiment and fluorescence imaging of intracellular Sn^{2+}, which **R1** accumulated in lysosomes and the acidity induced **R1** fluorescence emission. Furthermore, Sn^{2+} can also locate in lysosomes and enhanced the fluorescence of **R1** and **R2**. The more important, fluorescence of **R2** induced by Sn^{2+} and lysotracker overlapped very well, which indicates that **R2** can detection Sn^{2+} in lysosomes; at the same time fluorescence signal of **R2** demonstrated distribution of Sn^{2+} (Fig. 8, a2-d2). Over all, **R1** and **R2** were verified as lysosomes targeting and sensitive to Sn^{2+}. However, it is not sure that Sn^{2+} widely distributed in cell or accumulated in lysosomes.

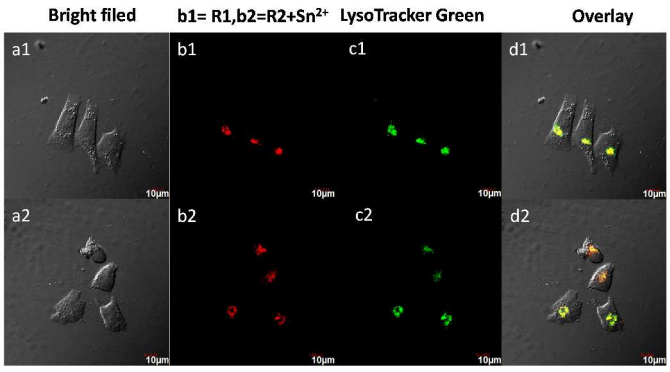

Fig. 8 CLSM images of KB cells. (a1- d1) Cells incubated with 10 μM **R1** and 1 μM LysoTracker Green for 30 min; (a2-d2) successively incubated with 10 μM **R2**, 50 μM SnF_2, 1 μM LysoTracker Green, each for 20 min. Emission was collected in red channel (b1, b2) at 560–660 nm (λ_{ex} = 543 nm) or in green channel at 500-540 nm (λex = 488 nm); a1, a2 are bright field images, and d1, d2 are overlay images, respectively.

To solve the problem mentioned above, comparative colocalization experiment was carried out. Firstly, the KB cells were stained with 50 μM Sn^{2+} at 37 ºC for 30 min, and then separately incubated with 10 μM **R1** and 1 μM LysoTracker® Green DND or **R2** and 1 μM LysoTracker® Green DND under the same conditions. As determined by CLSM, **R1** and **R2** gave fluorescence emission in a site of KB cells, which overlap with LysoTracker® Green DND very well (Fig. 9). There was no fluorescence in other site intracellular. This result indicats that Sn^{2+} is internalized into cells and leading to accumulation of the ions in lysosomes. This may be a transmission path of Sn. Many pharmaceutical agents, including various large and small molecules, must be delivered specifically to particular cell organelles in order to efficiently exert their therapeutic action. Such delivery is still mainly an unresolved problem, but targeting detection is a helpful attempt.[23]

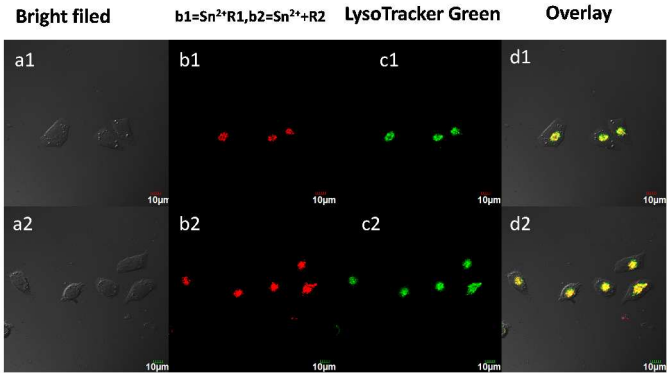

Fig. 9 CLSM images of KB cells. (a1- d1) Cells successively incubated with 50 μM SnF_2, 10 μM **R1** and 1 μM LysoTracker Green each for 20 min; (a2-d2) successively incubated with 50 μM SnF_2, 10 μM **R2** and 1 μM LysoTracker Green, each for 20 min. Emission was collected in red channel (b1, b2) at 560–660 nm (λ_{ex} = 543 nm) or in green channel at 500-540 nm (λ_{ex} = 488 nm); a1, a2 are bright field images and d1, d2 are overlay images, respectively.

Fluorescence imaging of Sn^{2+} in bacteria

It has been reported that Sn^{2+} can effectively inhibit streptococcus mutans.[1] We proceeded to investigate the

practical applicability of **R1** and **R2** as a Sn^{2+} probe in the fluorescence imaging of living streptococcus mutans (ATCC® 700610™). Firstly, the streptococcus mutans (ATCC® 700610™) were separately stained with 10 μM **R1** or **R2** at 37ºC for 60 min. As determined by CLSM, **R1** and **R2** gave no fluorescence emission without Sn^{2+} present (Fig. 10, a1-c1, a2-c2). When the streptococcus mutans were supplemented with **R1** or **R2** in the PBS for 60 min at 37 ºC and then incubated with 50 μM Sn^{2+} under the same conditions, **R1** and **R2** gave a significant fluorescence increasing (Fig. 10, d1-f1, d2-f2). The overlay of fluorescence and brightfield images revealed that the fluorescence signals were localized in the streptococcus mutans (ATCC® 700610™) (Fig. 10f1, f2), indicating that Sn^{2+} play its physiological role within bacteria.

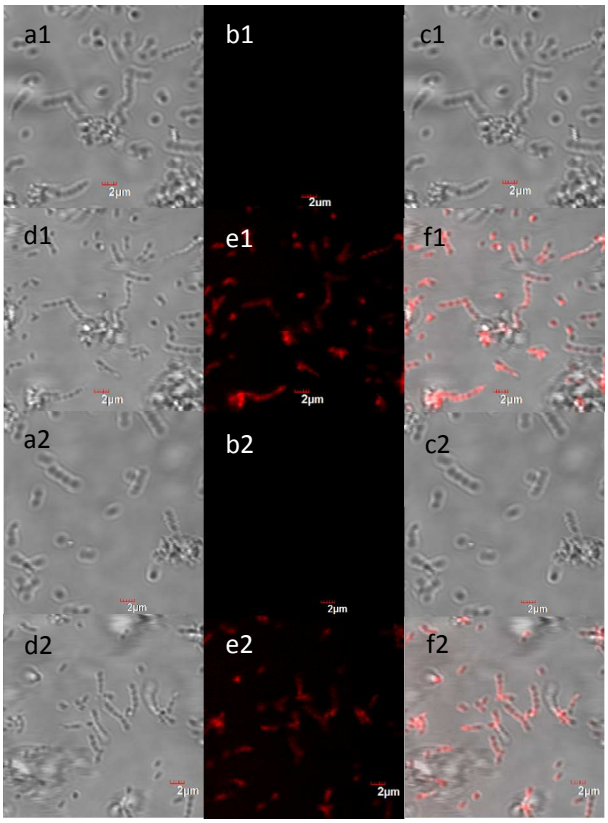

Fig.10 CLSM images of streptococcus mutans (ATCC® 700610™). (a1-c1) and (a2-c2) Cells separately incubated with 10 μM **R1** and **R2** for 30 min, respectively; (d1-f1) and (d2-f2) followed incubated with 50 μM SnF_2 for 30 min. Emission was collected in red channel at 560–660 nm (b1, e1, b2, e2); a1, d1, a2, d2 are bright field images and c1, f1, c2, f2 are overlay images, respectively (λ_{ex} = 543 nm).

Conclusion

To summarize, two chemosensors (**R1** and **R2**) for Sn^{2+} were synthesized and characterized. They all exhibit highly selectivity for Sn^{2+}, while **R2** shows more sensitive to Sn^{2+} than **R1**. In addition, **R2** is more suitable for detection Sn^{2+} in eukaryotic cell level, due to its low cytotoxicity, less background noise, particularly in more acidic environments like lysosomes. Application of **R1** and **R2** in eukaryotic cell level successfully image Sn^{2+} in streptococcus mutans (ATCC® 700610™). Furthermore, **R1** and **R2** as lysosomes tracker can demonstrate the distribution of Sn^{2+} in cells and bacteria, which is helpful to the research of pharmaceutical agent delivery and antibacterial mechanism of Sn^{2+}.

Acknowledgements

The authors thank for the financial support of the National Basic Research Program of China (2013CB733700), the China National Funds for Distinguished Young Scientists (21125104), National Natural Science Foundation of China (51373039), Program for Innovative Research Team in University (IRT1117), Program of Shanghai Subject Chief Scientist (12XD1405900), and Shanghai Leading Academic Discipline Project (B108).

Notes and references

[a] Department of Chemistry and Concerted Innovation Center of Chemistry for Energy Materials, Fudan University, 220 Handan Road, Shanghai 200433, China; email: yitao@fudan.edu.cn
[b] P&G Technology (Beijing) Co., Ltd. No.35 yuan Road, B zone, Shunyi District, Beijing, 101312 China.

Electronic Supplementary Information (ESI) available: [synthesis details and additional spectra]. See DOI: 10.1039/b000000x/

1 N. Tinanoff, *J. Clin. Dent*., 1995, **6** (Spec Issue), 37.
2 H. J. Keene, I. L. Shklair and G. J. Mickel, *J. Dent. Res.,* 1977, **56**, 21.
3 (a) H. Rudel, *Ecotoxicology and Environmental Safety,* 2003, **56**,180. (b) S. G. Schäfer and U. Femfert, *Regulatory Toxicology and Pharmacology*, 1984, **4**, 57.
4 N. Cardarelli, *Thymus*, 1990, **15**, 223.
5 L. R. Sherman, J. Masters and R. Peterson, *J. Anal. Toxicol*., 1986, **10**, 6.
6 S. Ulusoy, H. I. Ulusoy and M. Akcay, *Food Chem.,* 2012, **134**, 419.
7 M. Arvand, A. M. Moghimi, A. Afshari and N. Mahmoodi, *Anal. Chim. Acta.*, 2006, **579**, 102.
8 (a) X. R. Huang, W. J. Zhang, S. H. Han and X. Q. Wang, *Talanta*, 1997, **44**, 817. (b) T. Madrakian and F. Ghazizadeh, *J. Brazil Chem. Soc.,* 2009, **20**, 1535.
9 Q. Wang, C. Li, Y. Zou, H. Wang, T. Yi and C. Huang, *Org. Biomol. Chem*, 2012, **10**, 6740.
10 J. Liu, K. Wu, X. Li, Y. F. Han and M. Xia, *Rsc Advances*, 2013, **3**, 8924.
11 (a) S. K. Ko, Y. K. Yang, J. Tae and I. Shin, *J. Am. Chem. Soc.,* 2006, **128**, 14150. (b) J. Y. Kwon, Y. J. Jang, Y. J. Lee, K. M. Kim, M. S. Seo, W. Nam and J. Yoon, *J. Am. Chem. Soc.,* 2005, **127**, 10107.
12 S. Kenmoku, Y. Urano, H, Kojima and T. Nagano, *J. Am. Chem. Soc.,* 2007, **129**, 7313.
13 J. M. Sanfrutos, J. L. Jaramillo, M. O. Munoz, M. A. Fernandez, F. P. Balderas, F. H. Mateo and F. S. Gonzalez, *Org. Biomol. Chem.,* 2010, **8**, 667.

14 Y. Shiraishi, R. Miyamoto, X. Zhang and T. Hirai, *Org. Lett.*, 2007, **9**, 3921.
15 H. Yang, Z. Zhou, K. Huang, M. Yu, F. Li, T. Yi and C. Huang, *Org. Lett.*, 2007, **9**, 4729.
16 R. E. Melendez and W. D. Lubell, *J. Am. Chem. Soc.* 2004, **126**, 6759.
17 C. Y. Li, Y. Liu, Y. Q. Wu, Y. Sun and F. Y. Li, *Biomaterials*, 2013, **34**, 1223.
18 A. K. Mahapatra, S. K. Manna and D.Mandal, *Inorg. Chem.*, 2013, **52**, 10825.
19 R. L. Sheng, P. F. Wang, Y. H. Gao, Y. Wu, W. M. Liu, J. J. Ma, H. P. Li and S. K. Wu, *Tetrahedron*, 2010, **66**, 9655.
20 A. K. Mahapatra, S. K. Manna, D. Mandal and C. D. Mukhopadhyay, *J. Med. Chem.,* 1993, **36**, 1839.
21 (a) H. L. Li, J. L. Fan, F. L. Song, H. Zhu, J. J. Du, S. G. Sun and X. J. Peng, *Chem.-Eur. J*, 2010, **16**, 12349. (b) J. F. Zhang, Y. Zhou, J. Yoon, Y. Kim, S. J. Kim and J. S. Kim, *Org. Lett.*, 2010, **12**, 3852. (c) Z. X. Han, X. B. Zhang, L. Zhuo, Y. J. Gong, X. Y. Wu, J. Zhen, C. M. He, L. X. Jian, Z. Jing, G. L. Shen and R. Q. Yu, *Anal. Chem.*, 2010, **82**, 3108.
22 (a) Z. Li, Y. L. Song, Y. H. Yang, L. Yang, X. H. Huang, J. H. Han and S. F. Han, *Chem. Sci.*, 2012, **3**, 2941. (b) S. Q. Wu, Z. Li , J. H. Han and S. F. Han, *Chem. Commun.*, 2011, **47**, 11276. (c) I. Meerovich, A. Koshkaryev, R. Thekkedath and V. P. Torchilin, *Bioconjugate Chem.*, 2011, **22**, 2271.
23 L. Xue, G. P. Li, D. J. Zhu, Q. Liu and H. Jiang, *Inorg. Chem.*, 2012, **51**, 10842.

Graphic Abstract

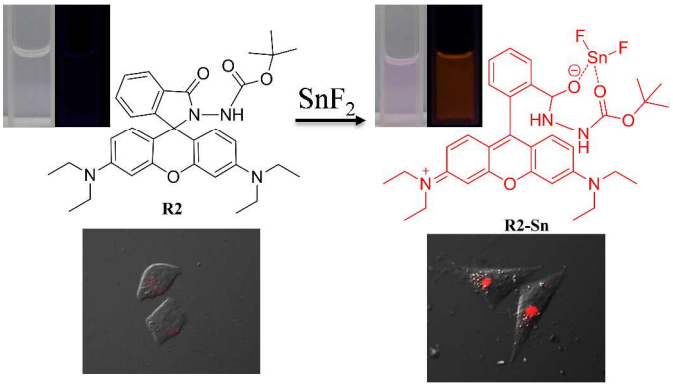

Fluorescent turning on probes for selective detection of Sn(II) in living eukaryotic and prokaryotic cells were developed.